Dyes and Pigments 95 (2012) 619–626

Contents lists available at SciVerse ScienceDirect

Dyes and Pigments

journal homepage: www.elsevier.com/locate/dyepig

Fluorescence and β-cyclodextrin inclusion properties of three carbazole-based dyes

Wenjian Lao [a,*], Cuihua Song [b], Jinmao You [b], Qingyu Ou [a]

[a] Lanzhou Institute of Chemical Physics, Chinese Academy of Sciences, Lanzhou 730000, Gansu, China
[b] School of chemistry and chemical engineering, Qufu 273165, Shandong, China

ARTICLE INFO

Article history:
Received 5 March 2012
Received in revised form
22 June 2012
Accepted 22 June 2012
Available online 9 July 2012

Keywords:
Carbazole derivative
Fluorescence property
Environmental effect
β-Cyclodextrin
Inclusion
Molecular dynamics simulation

ABSTRACT

Fluorescence behavior of three carbazole-based dyes, 2-(9H-carbazol-9-yl) butanoic acid, 2-(1,4-dimethyl-9H-carbazol-9-yl)acetic acid and 3-(1,4-dimethyl-9H-carbazol-9-yl)propanoic acid were examined. General solvent effects of the butanoic and acetic acid derivatives in 23 different solvents was not well-described by the Lippert–Mataga equation, indicating a specific solvent effect due to intermolecular hydrogen bonding dominated fluorescence spectra. The emission wavelengths and fluorescence intensities were relatively stable in aqueous acetonitrile and aqueous methanol solutions. Their fluorescence intensities increased from low to high pH and also from high to low temperature. The acid dissociation constants of the three carbazole derivatives in their ground state were estimated to be in the range 3.2–4.8. The fluorescence intensities were also enhanced in the presence of β-cyclodextrin. The average stability constant of the inclusion complexes was 21.2 ± 13.4 at pH3 and 54.0 ± 7.0 at pH8. A molecular dynamics simulation indicated that the carbazole moiety was partially included into the β-cyclodextrin cavity leaving the carboxylic acid group exposed.

1. Introduction

Carbazole-based dyes have exhibited excellent optical and electrical properties as well as pharmacological activities. A large number of carbazole derivatives have been synthesized and characterized, and diverse organic materials and electronic devices based on these derivatives have been prepared and evaluated [1–3]. Highly stable and fluorescent compounds containing a carbazole moiety were examined as probe and tag to sense variation of pH, temperature, polarity and/or microviscosity in various microenvironments such as supramolecular host cavities, micelles, polymers, and biomolecules [4]. A few carbazole-based fluorescent derivatization reagents were evaluated and utilized in high-performance liquid chromatography (HPLC), because of high adaptability with the mobile phase system [5]. Necessarily, environmental effects, e.g., solvent component, pH, and temperature, on fluorescence properties were investigated to optimize manipulation for the derivatization reagents. For instance, You et al. firstly studied the fluorescent behavior for several carbazole derivatization reagents including carbazole-9-yl-acetic acid and carbazole-9-yl-propanoic acid that were used in the measurement of amino acid and bioamine [6–8]. Fluorescent behavior of these reagents was investigated in different mobile phase modifiers, temperature, pH, halogen-salts, organic halides, heavy atoms, surfactants, and cyclodextrin (CD). Later, Romero-Ale et al. further evaluated effect of the environmental factors such as different solvents, buffered aqueous solution, modified CDs, on fluorescent behavior for some carbazole compounds [9]. They verified that the inclusion interaction in the CD cavity could change the reactivity of the carbazole derivatization reagent [10].

Although there have been plenty of developed dyes, preparation and characterization of new fluorescence reagents is always an attractive field. We have synthesized several new carbazole derivatives for potential application as fluorescent tags [11]. Among them, 2-(1,4-dimethyl-9H-carbazol-9-yl)acetic acid (DCAA), 3-(1,4-dimethyl-9H-carbazol-9-yl) propanoic acid (DCPA) with two methyl substituents on carbazole ring were expected to have strong fluorescence intensity and to become alternative choice of derivatization reagent for achieving better chromatographic separation of the derivatives (Scheme 1) [12,13]. Another reagent, 2-(9H-carbazol-9-yl) butanoic acid (CBA), possessing a chiral center in the structure was considered to be a probe in asymmetric environment [14,15]. Their chemical structures have been fully characterized, but fluorescence properties have not been well investigated.

The goal of this study is to investigate fluorescence properties of the three carbazole compounds (CBA, DCAA and DCPA). Three

* Corresponding author. Present address: 101 Pergola, Irvine, CA 92612, USA. Tel.: +1 949 394 6378; fax: +1 949 748 7008.
E-mail address: laowjbj@hotmail.com (W. Lao).

0143-7208/$ – see front matter © 2012 Elsevier Ltd. All rights reserved.
http://dx.doi.org/10.1016/j.dyepig.2012.06.015

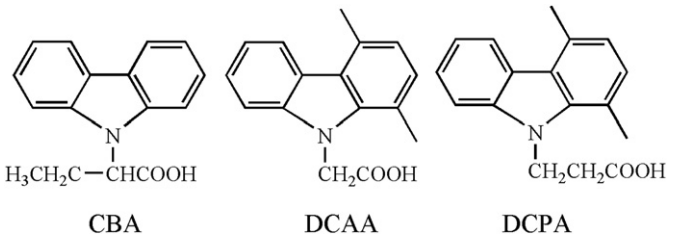

Scheme 1. Chemical structures of the carbazole compounds.

aspects of task were conducted. First, fluorescence behavior was examined in different solvents, HPLC mobile phases, pH values, and temperatures, so as to establish related fluorescent and molecular parameters. Second, variation of fluorescence behavior was evaluated due to inclusion interaction with β-CD. The stability constant of the inclusion complex was estimated through the fluorescent measurement. Lastly, host-guest orientation in the complex was simulated by molecular dynamics to explain the inclusion interaction and therein the inclusion model could be proposed. Results of this study should be useful information for further development of carbazole-based fluorescence dyes.

2. Material and methods

2.1. Materials

The 2-(9H-carbazol-9-yl) butanoic acid (CBA), 2-(1,4-dimethyl-9H-carbazol-9-yl)acetic acid (DCAA), 3-(1,4-dimethyl-9H-carbazol-9-yl) propanoic acid (DCPA) were synthesized by microwave irradiation method described previously (Scheme 1) [16]. β-Cyclodextrin (β-CD) was purchased from YuNan Gourmet Factory (Guang Dong, China), and was purified by recrystallization in double-distilled water twice. All other reagents and solvents were analytical grade or better. Ultraviolet–visible (UV–vis) absorption spectra were recorded with a Hitachi 330 UV–Vis spectrophotometer (Japan). Fluorescence excitation and emission spectra were obtained on a Hitachi 650-10S spectrofluorimeter (Japan). Standard rectangular quartz cuvette (1-cm pathlength) was used in the measurements.

2.2. Influence of solvent, pH and temperature on native fluorescence

A stock solution of the individual carbazole compound was prepared at 5.0×10^{-3} mol/L level in acetonitrile. For evaluation of solvent effect, 2 μL of the stock solution was transferred into a dry quartz cell; once after the solvent was evaporated, 2 mL of appropriate solvent was added to make solution at 5.0×10^{-6} mol/L in room temperature (22 ± 1 °C). Twenty-three pure solvents (including hexane, cyclohexane, toluene, diethyl ether, ethyl acetate, acetic acid, methylene chloride, benzene, tetrahydrofuran, 1-octanol, 1-heptanol, 1-hexanol, 1-pentanol, 1-butanol, 1-propanol, ethanol, methanol, acetonitrile, acetone, chloroform, dimethyl sulfoxide, N,N-dimethylformamide (DMF), and water), and two series of mixture solutions (acetonitrile–water and methanol–water mixture in different volume concentrations with 10% stepwise increment) were examined. For evaluation of pH effect, 2 mol/L of sodium acetate aqueous solution was used as buffer. In the cell, 10 μL of the stock solution was transferred into 2 mL of the buffer solution to yield 2.5×10^{-5} mol/L solution at room temperature ($\approx 22 \pm 1$ °C). For evaluation of temperature effect, the fluorescence spectra were separately recorded at four temperatures (20, 35, 50, and 65 °C) for the carbazole compounds at 5.0×10^{-6} mol/L in pure 1-pentanol and in the sodium acetate buffer solution at pH3.0 and pH8.0.

2.3. Inclusion interaction with β-CD

Stock solution of β-CD was prepared at 0.1 mol/L level in double-distilled water. Concentration of the carbazole compound was prepared at 5×10^{-6} mol/L in the cell. The inclusion interaction was evaluated with excitation wavelength of 292 nm and emission wavelength of 368 nm at 25 °C for two pH values (pH = 3.0 or 8.0). The molecular dynamics simulations were performed using Chem3D Pro software (Cambridge Soft, Cambridge, MA, USA). The geometry optimized model of carbazole compounds and β-CD were energy-minimized by molecular mechanics using MM2 force field. The carboxylic acid group on the carbazole compounds was set in undissociated and dissociated form. The settings in molecular dynamics calculation were 2 fs of step interval, and 1 kcal/atom/ps of heating/cooling rate. The simulation was terminated when a stable conformation was achieved. Statistics analysis (*t*-test) employed SigmaStat software (V2.03, SPSS).

3. Results and discussion

3.1. Influence of solvent, pH and temperature on native fluorescence

The carbazole compounds showed an ambiguous general solvent effect. The excitation and emission wavelengths had small shifts among the carbazole compounds in acetonitrile (Table 1), whereas fluorescence intensities were barely changed by the alkyl substituent on the aromatic ring and by the carboxyl acid group on the nitrogen atom. The effect of solvent on the fluorescence spectra was examined for CBA and DCAA in 23 solvents with different polarity and dielectric constant. The excitation and emission wavelengths were in the ranges of 336–345 nm and 344–358 nm for CBA, 334–344 nm and 346–366 nm for DCAA, respectively. The solvent effect was characterized by the Lippert–Mataga equation (Eq. (1)).

$$\Delta\nu = \overline{\nu_a} - \overline{\nu_f} = \frac{2}{hc}\left(\frac{\varepsilon - 1}{2\varepsilon + 1} - \frac{n^2 - 1}{2n^2 + 1}\right)\frac{(\mu^* - \mu)^2}{a^3} + \text{constant} \quad (1)$$

$$\Delta f = \frac{\varepsilon - 1}{2\varepsilon + 1} - \frac{n^2 - 1}{2n^2 + 1} \quad (2)$$

where $\Delta\nu = \overline{\nu_a} - \overline{\nu_f}$ is the Stokes shift of the absorption and emission band maxima; h is Planck constant; c is the velocity of light; μ^* and μ are the dipole moments of the excited state and ground state; a is the radius of the cavity in which the solute resides; ε is the dielectric constant of the solvent; n is the refractive index of the solvent; Δf is the orientation polarizability representing a measure of the solvent polarity and polarizability. The Lippert–Mataga plots of these two compounds did not show a linear relationship ($R^2 = 0.18$ for CBA, $R^2 = 0.13$ for DCAA) between $\Delta\nu$ and Δf, indicating weak influence from general solvent effect, i.e., non-specific type of interaction, between the carbazole compounds and solvent on the fluorescence spectra (Fig. 1). However, the general trend still exhibited positive correlation between Stokes shifts and Δf. Both

Table 1
Absorbance and fluorescent parameters of the carbazole compounds.

Compound.	λ_{ab} (nm)	λ_{em} (nm)	Stokes shift (cm^{-1})
CBA	290_{max}, 338	348_{max}, 362	850
DCAA	287_{max}, 338	349_{max}, 363	933
DCPA	287_{max}, 342	353_{max}, 368	911

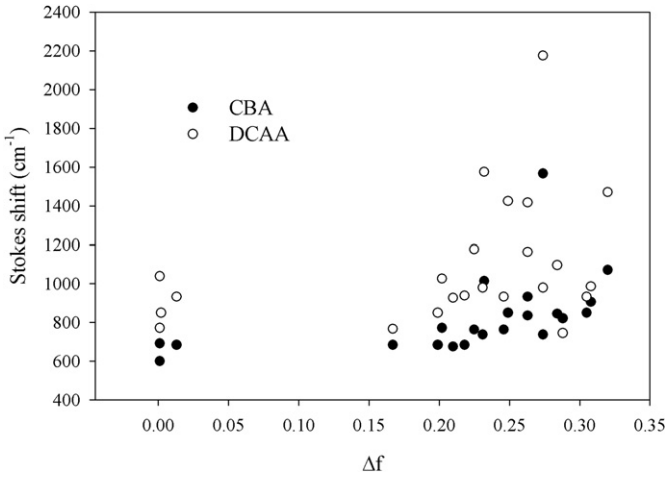

Fig. 1. Lippert–Mataga plots of CBA and DCAA.

CBA and DCAA presented the longest emission wavelengths (358 and 366 nm) and largest Stokes shifts (1566 and 2176 cm^{-1}) in DMF. Adding 1% (v/v) of DMF into DCAA–hexane solution made obvious changes in emission wavelength and fluorescence intensity, illustrating specific solvent–solute interaction (Fig. 2). The position of two of the emission bands at 346 and 361 nm, respectively, had 2 and 3 nm redshifts with 31% and 42% enhancements in fluorescence intensity. This was comparable to the 35% difference of DCAA fluorescence intensity between the hexane and the DMF solutions. The carboxyl acid group on the carbazole moiety may form intermolecular hydrogen bond with each other and/or solvent molecule in solution, which could stabilize the excited state to generate the specific solvent interaction [9,17].

The emission wavelength and fluorescence intensity presented slight variations in the commonly used HPLC mobile phases such as acetonitrile–water and methanol–water system. The emission wavelengths in the acetonitrile solutions were 8, 10, and 6 nm shorter than in water for CBA, DCAA, and DCPA, respectively, but the emission wavelengths were almost identical in the water and the aqueous mixed solutions. The emission wavelengths in methanol solution were only 4 nm shorter than in water for DCAA and DCPA, and no change for CBA. The maximum excitation wavelengths remained identical in the acetonitrile–water and methanol–water systems. Relative fluorescence intensities were changeable along with the solvent ratio, but the magnitude of the variance was below 20% (Fig. 3). All the three compounds exhibited relative stable fluorescence behaviours in the acetonitrile–water

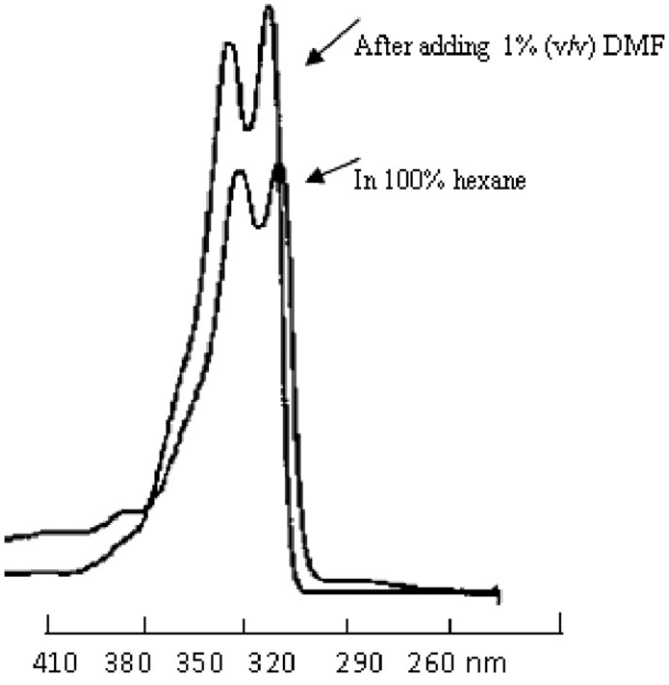

Fig. 2. Effect of DMF addition (1%, v/v) to DCAA fluorescence spectra in hexane.

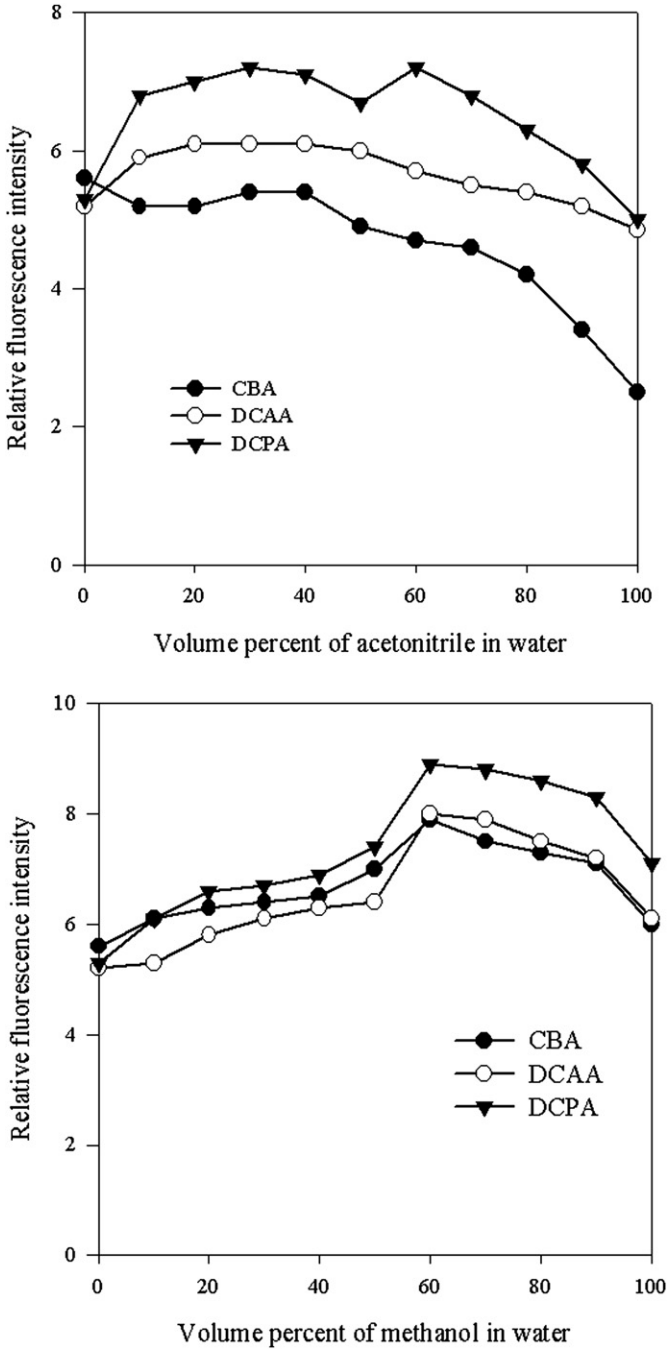

Fig. 3. Profiles of fluorescence intensity in acetonitrile–water (up) and methanol–-water mixtures.

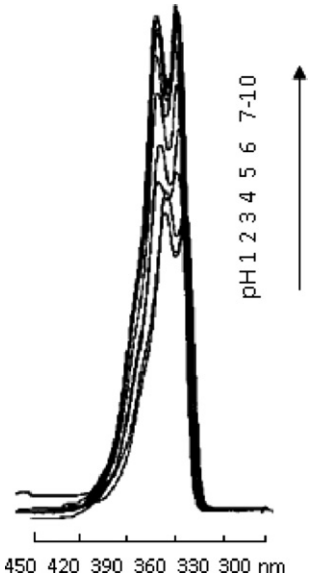

Fig. 4. Effect of pH on CBA fluorescence spectra in sodium acetate buffer solutions.

and methanol–water systems so that they were appropriate for utilization as derivatization reagent [18].

Fluorescence quantum yields (ϕs) of DCAA and DCPA, previously measured against carbazole in acetonitrile, were identical and approximately equal to carbazole's [13]. The fluorescence quantum yields of 2-(9H-carbazol-9-yl) acetic acid (CAA), 3-(9H-carbazol-9-yl) propanoic acid (3-CPA), and 2-(9H-carbazol-9-yl) propanoic acid (2-CPA), which are structurally similar to the compounds in the present study, were measured against quinine sulfate ($\phi = 0.55$) to be approximately identical 0.36 in acetonitrile, whereas 0.26 for CAA and 3-CPA, 0.32 for 2-CPA in methanol [18]. They decreased 32 ± 13% and 10 ± 2% in 1:1 (v/v) of acetonitrile–water and methanol–water solutions, respectively. Considering the structural similarity, it was believed DCAA, DCPA and CBA should have comparable trend in variation of the fluorescence quantum yield, which the fluorescence quantum yields were larger in acetonitrile than in methanol, and declined in the solutions of aqueous mixtures.

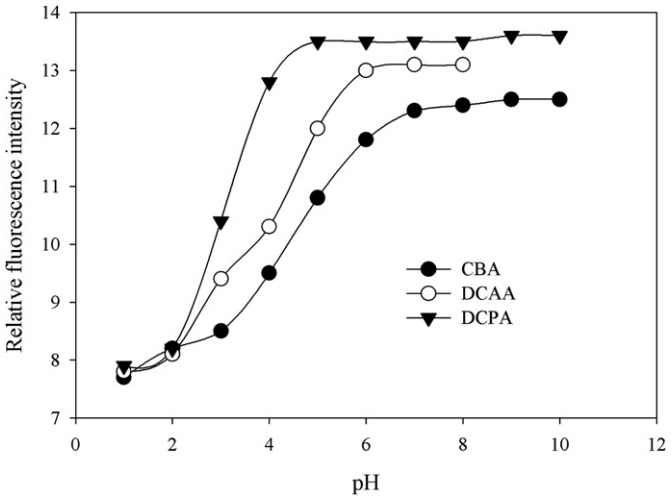

Fig. 5. Profiles of fluorescence intensity at different pH values.

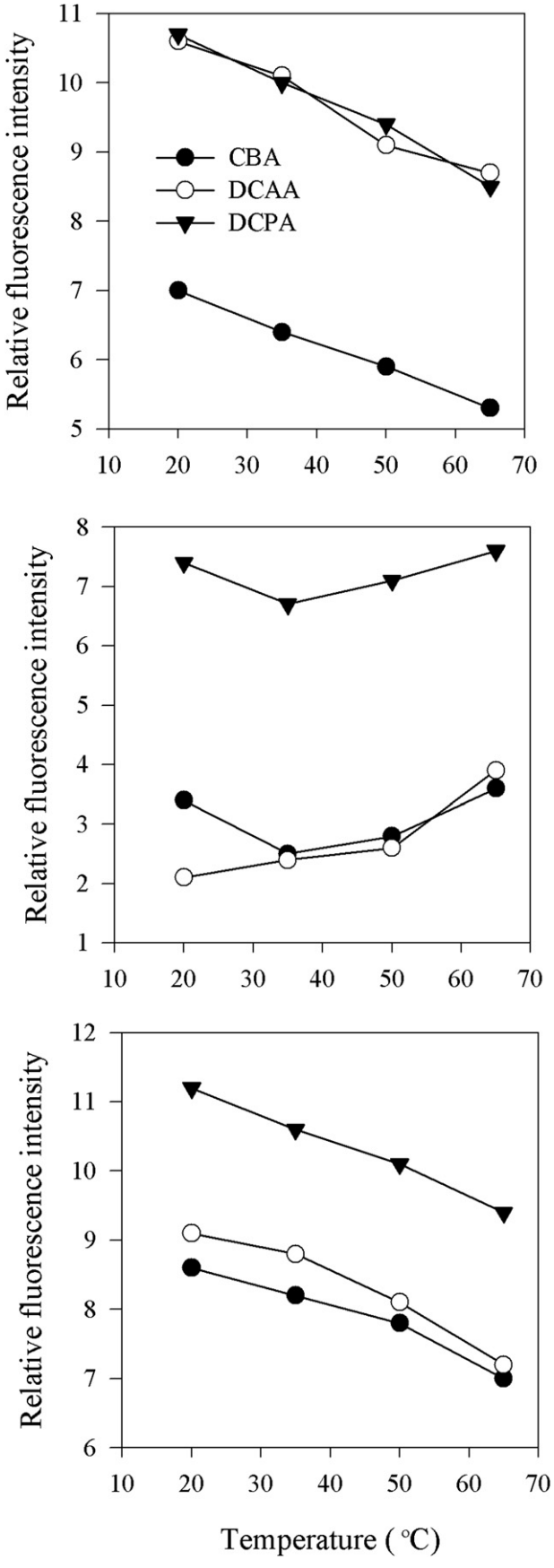

Fig. 6. Effect of temperature on fluorescence intensity in 1-pentanol and sodium acetate buffer solutions at pH3 and pH8.

Table 2
Percent enhancement of fluorescence intensity in presence of β-CD at different concentrations, pH values, and relative enhancement (pH3/pH8). The concentration of carbazole compounds in the media was 5.0×10^{-6} mol/L.

β-CD (mol/L)	CBA			DCAA			DCPA		
	pH3	pH8	pH3/pH8	pH3	pH8	pH3/pH8	pH3	pH8	pH3/pH8
0.0010	9.6	3.0	3.2	5.4	7.7	0.70	15.4	4.8	3.2
0.0020	21	9.0	2.3	9.0	15	0.60	22	10	2.2
0.0039	40	16	2.5	20	21	0.95	38	18	2.1
0.0057	54	18	3.0	29	32	0.91	58	24	2.4
0.0074	87	26	3.3	38	45	0.84	66	27	2.4
0.0091	102	37	2.8	54	59	0.92	83	31	2.7
0.0107	121	48	2.5	61	65	0.94	118	48	2.5
Ave ± std			2.8 ± 0.4			0.8 ± 0.1			2.5 ± 0.4

The emission wavelength and fluorescence intensity were affected by pH in aqueous buffer solution. The carbazole compounds emitted fluorescence in acidic and dissociation forms, while the emission wavelength had a redshift and fluorescence intensity increased from low to high pH values (Figs. 4 and 5). The redshifts were 6, 5, and 4 nm for CBA, DCAA, and DCPA, respectively, from the acidic to the dissociation form with a negligible shift in excitation wavelength. Their acid dissociation constants (pK_a) in ground state were 4.32 (CBA), 4.81 (DCAA), and 3.20 (DCPA) estimated by Henderson–Hasselbach equation (Eq. (3)).

$$\mathrm{pH} = pK_a + \log\frac{I - I_{\min}}{I_{\max} - I} \tag{3}$$

where I is the fluorescence intensity, $I_{\min}$ is the minimum fluorescence intensity in acidic form; $I_{\max}$ is the maximum fluorescence intensity in basic form. Their acid dissociation constants in excited state (pK_a^*) were further calculated by the Förster equation (Eq. (4)).

$$pK_a^* = pK_a - hc\Delta\bar{\nu}/2.3RT \tag{4}$$

where $\Delta\bar{\nu}$ is the wavenumber difference of transition energy between acidic and basic forms; R is the ideal gas constant; T is the temperature. The pK_a^* values calculated as 3.31 (CBA), 3.96 (DCAA), and 2.56 (DCPA) were smaller than the corresponding pK_a indicating their stronger acidity in the excited state. For comparison, pK_a of another two carbazole acids were carbazole-9-yl-acetic acid (6.33) [6] and 2-hydroxy-9H-carbazole-1-carboxylic acid (3.55) [19]. The pK_a of dibenzofuran-2-carboxylic acid, a non-carbazole compound, in the ground and first electronic excited states were $pK_a = 4.19$ and $pK_a^* = 8.5$ [20].

The fluorescence intensity decreased at elevated temperature without significant emission wavelength shift (Fig. 6). In 1-pentanol and the aqueous buffer solution at pH 8, the fluorescence intensities of the three compounds were described by the following equation (Eq. (5)).

$$\ln\left(\frac{I_0 - I}{I}\right) = -\frac{E_a}{RT} + \text{constant} \tag{5}$$

where I_0 is the fluorescence intensity at the lowest experimental temperature (293 K in this study); E_a is the activation energy [21]. The E_a for CBA, DCAA, and DCPA were 35.5 ($r = 0.9992$), 37.7($r = 0.9504$), and 43.2 ($r = 0.9999$) kJ/mol in 1-pentanol, 44.5 ($r = 0.9988$), 59.3 ($r = 0.9929$), and 35.2 ($r = 0.9999$) kJ/mol in the buffer solution at pH 8, respectively. In the buffer solution at pH 3, the fluorescence intensity variation displayed conjoined effects of temperature and dissociation. Shown in Fig. 6, the fluorescence intensity for CBA and DCPA decreased from 25 to 35 °C, and then turned to gradual increase at higher temperature, whereas the DCAA fluorescence intensity only exhibit upward trend. These properties could make them potentially applicable as an environmental probe [22].

3.2. Inclusion interaction with β-CD

The fluorescence intensities of the three compounds enhanced in the presence of β-CD. The enhancement of the fluorescence intensity increased along with increasing β-CD concentration in both pH3 and pH8 systems, indicating at least partial carbazole fluorophore was included within the β-CD cavity to form a complex (Table 2). The enhancement for CBA and DCPA was up to 2 times larger at pH3 than at pH8, while no difference ($p = 0.734$) for DCAA in the two pH values. In contract, it was reported that 9-carbazolylacetic acid only had small enhancements of the fluorescence intensity in buffered aqueous solutions (1.3% at pH 4.5 and 6.2% at pH 8.8) with host of 2-hydroxypropyl-β-CD (HP-β-CD) [9]. These data imply that CBA and DCPA were more sensitive in respect of the inclusion interaction within the β-CD concentration range in the present study.

The complex stability constant (K_s, L/mol) can be estimated by using the Benesi–Hildebrand equation from double reciprocal plots as given by the following equation.

$$\frac{1}{F - F_0} = \frac{1}{K_s \times \Delta E \times G_0 \times \mathrm{CD}_0} + \frac{1}{\Delta E \times G_0} \tag{6}$$

where F is the complex fluorescence intensity; F_0 is the fluorescence intensity in absence of β-CD; ΔE signifies difference of molar fluorescence intensity between the free guest and complex; G_0 is the guest nominal concentration; CD_0 denotes β-CD concentration (the host). Fitting with the fluorescence intensity and β-CD concentrations in Eq. (6) to calculate K_s value showed very high correlation coefficients ($r^2 > 0.99$) for each of the carbazole compounds at pH3 and pH8. Consequently, 1:1 complex stoichiometry in the inclusion was deduced (Table 3). The K_s values generally were greater at pH8 than at pH3 for all the three compounds because the average K_s, i.e., 21.2 ± 13.4 at pH3 and 54.0 ± 7.0 at pH8, had 2.5-fold difference. Moreover, the K_s values increased in order of DCAA > DCPA > CBA at pH3, but at pH8, all the K_s values actually were not different.

The guest percent molar fraction in the complex (M_f%) provided further insight into the inclusion interaction. The M_f% was estimated by the following equation [23]:

$$M_f\% = \left(1 - \frac{1}{1 + K_s \times \mathrm{CD}_0}\right) \times 100 \tag{7}$$

Table 3
Stability constant (K_s, L/mol) of 1:1 inclusion complex between carbazole compound and β-CD, and Gibbs free energy change ($-\Delta G^\circ$, kJ/mol) at 25 °C.

	CBA		DCAA		DCPA	
	K_s	$-\Delta G^\circ$	K_s	$-\Delta G^\circ$	Ks	$-\Delta G^\circ$
pH = 3	9.7 ± 0.4	5.63	36 ± 5.5	8.87	18 ± 0.8	7.16
pH = 8	57 ± 6.9	10.0	59 ± 8.0	10.1	46 ± 6.1	9.48

Table 4
Molar fraction of carbazole compound (M_f %) in 1:1 inclusion complex at 25 °C and M_f ratio (pH8/pH3).

β-CD concentration (mol/L)	CBA			DCAA			DCPA		
	pH = 3	pH = 8	pH8/pH3	pH = 3	pH = 8	pH8/pH3	pH = 3	pH = 8	pH8/pH3
0.00099	0.95	5.34	5.62	3.44	5.52	1.60	1.75	4.36	2.49
0.00196	1.87	10.1	5.40	6.59	10.4	1.57	3.41	8.27	2.43
0.00385	3.60	18.0	5.00	12.2	18.5	1.52	6.48	15.1	2.33
0.00566	5.20	24.4	4.69	16.93	25.0	1.48	9.25	20.7	2.24
0.00741	6.71	29.7	4.43	21.1	30.4	1.44	11.8	25.4	2.15
0.00909	8.10	34.1	4.21	24.7	34.9	1.41	14.1	29.5	2.09
0.01070	9.40	37.9	4.03	27.8	38.7	1.39	16.2	33.0	2.04
Ave ± std			4.76 ± 0.60			1.49 ± 0.08			2.25 ± 0.17

The M_f% values became greater with increasing β-CD concentration for all the three compounds at the both pH values (Table 4). There were more molecules involved in the complex from pH3 to pH8 for CBA ($p = 0.004$) and DCPA ($p = 0.040$), but statistically same amount of DCAA molecules were included in β-CD ($p = 0.239$) at the both pH values. At pH8, amount of molecules associated with β-CD had no difference for the three guest compounds. These indicated more guest molecules associated with β-CD at higher host concentration.

The structural factor of the three carbazole compounds determined the different behavior in the inclusion interaction. Apparently, there are two major structural differences among the three carbazole compounds, i.e., the methyl substituent on carbazole ring and carboxyl acid group on the nitrogen atom, which resulted in their different pK_a values. At pH8, carboxyl acid group was all in dissociation form, leading to identical and greater K_s and M_f% than at pH3 for all three compounds. Therefore, the differences in structure and pK_a did not differentiate the inclusion interaction at pH8, implying the inclusion mechanism was most likely similar for all the three compounds. At pH3, even though the dissociation degree of DCPA ($pK_a = 3.20$) was smaller than that of CBA ($pK_a = 4.32$), the K_s of DCPA was larger than that of CBA. It revealed that the longer side-chain structure of carboxyl group implemented stronger restriction to the inclusion interaction than the effect of acid dissociation. It should also be noticed that the two methyl groups on carbazole ring might increase additional hydrophobicity for DCAA and DCPA to favor their inclusion interactions.

The K_s values for cyclodextrin complexes ranged from 0 to approximately 100,000 reported in the literature; mean K_s values of pharmaceutical compounds and β-CD were statistically estimated to be 490 [24]. Very weak bindings are roughly characterized as $K_s < 500$. Comparably, the carbazole compounds were very weakly included in β-CD cavity. The K_s for carbamazepine inclusion in HP-β-CD was 650, for naproxen in β-CD was 1378. Carbamazepine has a three-ring structure with a short N-methyl amide substituent that likely did not make significant hindrance to the inclusion [25]. Being structurally smaller than carbazole, naproxen has a α-methyl acetic acid group on naphthalene meriting the larger K_s [26]. We previously reported N-acetic acid group was almost perpendicular to carbazole-ring plane in X-ray crystal structure of 2-(3-Br-9H-carbazol-9-yl) acetic acid [27]. It was reasonable to believe that the three carbazole compounds in the present study should have similar configurations. Therefore, the steric hindrance by the substituent on carbazole nitrogen atom seems to be responsible for the weak binding.

3.3. Molecular dynamics simulation

In order to better understand the inclusion interaction, complex formation was simulated by molecular dynamics. Two initial models were adopted with carbazole ring in parallel and perpendicular directions relative to β-CD cavity (Fig. 7). As an example, stereo initial docking models of DCAA-β-CD were presented in Fig. S1 of Supplementary material. Through the simulation, the resulting complex structures showed the carbazole moiety partially included into the β-CD cavity in inclined direction to maximize the inclusion leaving the carboxylic group outside. A representative complex model of DCAA-β-CD at pH3 is exhibited in Fig. 8, while other models for the three compounds at pH 3 and pH8 are shown in Supplementary material (Fig. S2–S6). The resulting complex structures were similar for the three compounds in both undissociated and dissociated forms from the two initial models. Specially for DCAA and DCPA, the benzene ring with methyl group was mostly included into β-CD cavity. On the basis of the simulation results, a generic inclusion model was proposed (Fig. 8).

The molecular dynamics simulation was beneficial to understand the inclusion interaction [28]. The atom distances between carbonyl oxygen and hydroxyl hydrogen of β-CD were <2 nm for CBA and DCAA, and >3.5 nm for DCPA, implying that a hydrogen bond could be formed in the inclusion complex for CBA and DCAA, but unlikely for DCPA. It was probably due to shorter chain length of acetic acid group on CBA and DCAA more facilitating hydrogen-bond formation. At pH 3, the hydrogen bond did not promote the K_s value of CBA over DCPA, which revealed the steric hindrance from substituent on the nitrogen atom played a more important role in reducing the inclusion interaction. The simulation also exhibited the ameliorative function of the methyl groups to the inclusion because of more affinity to β-CD hydrophobic cavity. On the other hand, the simulation showed β-CD conformation was changed from perfectly round shape before

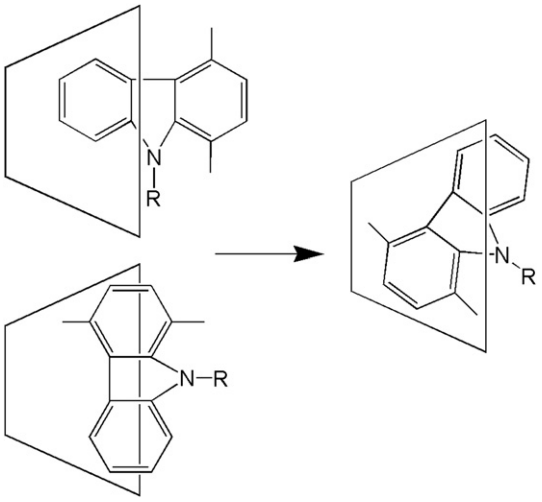

Fig. 7. Initial docking patterns for molecular dynamics simulation (left) and proposed generic inclusion model (right).

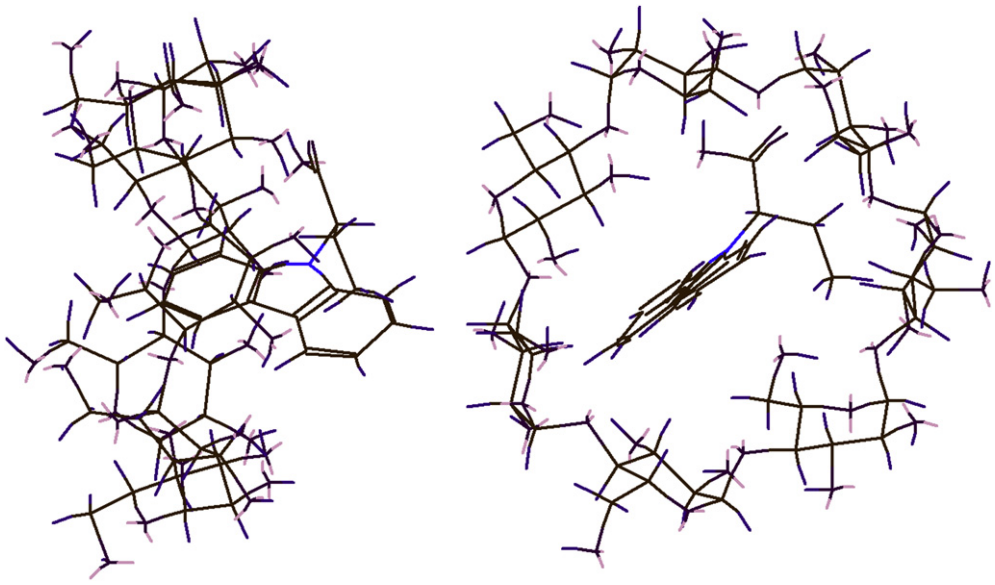

Fig. 8. The equilibrium structure of DCAA and β-CD inclusion complex at pH3 from the molecular dynamics simulation. Left, side view; right, view from face of β-CD secondary hydroxyl groups.

the inclusion interaction to ellipse shape in the complex. This was consistent with former studies on β-CD conformational flexibility [28,29].

4. Conclusions

Solvent influence illustrated by Lippert–Mataga plots was primarily dominated by a specific type of interaction such as an intermolecular hydrogen bond. The florescence emissions of the three compounds were relatively stable in the acetonitrile–water and methanol–water solvent systems to be suitable for application as derivatization reagents. Their florescence intensities were sensitive to pH and temperature deviations, making them usable as environmental probes. The sensitive feature was further illustrated by the β-CD inclusion interaction. The fluorescence intensities were evidently enhanced by forming a complex, although the K_s values were not high ($<$60). The steric hindrance from N-substitution was considered to cause the weak binding. Through molecular dynamics simulation, an inclusion pattern was proposed to help explain the inclusion interaction.

Acknowledgments

This work was supported by the Director Foundation of Lanzhou Institute of Chemical Physics, Chinese Academy of Sciences, and the National Natural Science Foundation of China (29870533).

Appendix A. Supplementary material

Supplementary material associated with this article can be found, in the online version, at doi:10.1016/j.dyepig.2012.06.015.

References

[1] Weber L, Halama J, Werner V, Hanke K, Bohling L, Chrostowska A, et al. Synthetic, structural, photophysical and computational studies on pi-conjugated 1,3,2-benzodiazaboroles with carbazole building blocks. Eur J Inorg Chem 2010;34:5416–25.
[2] Takagi K, Takao H, Nakagawa T. Synthesis and characterization of nitrogen-linked carbazole-containing fluorescent polymers. J Polym Sci Part A Polym Chem 2010;48(17):3729–35.
[3] Gupta VD, Padalkar VS, Phatangare KR, Patil VS, Umape PG, Sekar N. The synthesis and photo-physical properties of extended styryl fluorescent derivatives of N-ethyl carbazole. Dyes Pigments 2011;88(3):378–84.
[4] Sarkar A, Chakravorti S. A solvent-dependent luminescence study on 9-phenyl carbazole. J Lumin 1998;78(3):205–11.
[5] Shi YW, Ming YF, Wang CP, Zhao X, Zhang R, You JM. Determination of amino acids from hydrolyzed bovine serum albumin by high-performance liquid chromatography-mass spectrometry with fluorescence and electrospray ionization detection. Chin J Anal Chem 2006;34(4):503–7.
[6] You YM, Sun HT, Lao WJ, Ou QY. Fluorescence properties of carbazole-9-yl-acetyl chloride and its application for the simultaneous determination of amino acids and biogenic amines via liquid chromatography with fluorescence detection. Anal Chim Acta 1999;382(1–2):51–65.
[7] You JM, You J, Lao WJ, Wang GJ, Jia XG. Fluorescence properties of carbazole-9-ylpropionic acid and its application to the determination of amines via HPLC with fluorescence detection. Analyst 1999;124(3):281–8.
[8] You JM, Sun XJ, Lao WJ, Ou QY. Determination of alcohols using condensation agent carbazole-9-acetyl-benzene-disulfonate by high performance liquid chromatography with pre-column fluorescence derivatization. Chromatographia 1999;49(11–12):657–65.
[9] Romero-Ale EE, Olives AI, Martin MA, del Castillo B, Lopez-Alvarado P, Menendez JC. Environmental effects on the fluorescence behaviour of carbazole derivatization reagents. Luminescence 2005;20(3):162–9.
[10] Olives AI, Romero-Ale EE, Martin MA, del Castillo B, Lopez-Alvarado P, Menendez JC. Changes in the reactivity of the fluorescent reagents carbazole-9-carbonyl chloride and 9-carbazolylacetic acid in the presence of cyclodextrins. J Incl Phenom Macro 2007;57(1–4):553–9.
[11] Lao WJ, You JM, Sun XJ, Kong XH, Ou QY. Facile and rapid synthesis of 9H-carbazole-9-carboxylic acids under microwave irradiation. Synth Commun 2000;30(19):3491–9.
[12] You JM, Shi YW, Zhao XN, Zhang HF, Suo YR, Li YL, et al. Enhancement of atmospheric pressure chemical ionization for the determination of free and glycine-conjugated bile acids in human serum. J Sep Sci 2006;29(18):2837–46.
[13] Lao WJ, Sun XJ, You JM, Ou QG. Microwave-assisted rapid preparation of substituted carbazole-9-acetic and propionic acids and their absorption and fluorescence spectra. Monatsh Chem 2000;131(7):803–11.
[14] Lao WJ, Yu ZW, Liu YQ, Ou QY. Microwave-induced fast synthesis and optical resolution of 9H-carbazole-2-carboxylic acids enantiomers. J Prakt Chem 2000;342(6):596–8.
[15] Wu YB, Guo HM, James TD, Zhao JZ. Enantioselective recognition of mandelic acid by a 3,6-dithiophen-2-yl-9H-carbazole-based chiral fluorescent bisboronic acid sensor. J Org Chem 2011;76(14):5685–95.
[16] Mallik AK, Shingo K, Gautam UG, Sawada T, Takafuji M, Ihara H. Complete chromatographic separation of steroids, including 17 alpha and 17 beta-estradiols, using a carbazole-based polymeric organic phase in both reversed and normal-phase HPLC. Anal Bioanal Chem 2010;397(2):623–9.
[17] Hashemi J, Alizadeh N. Investigation of solvent effect and cyclodextrins on fluorescence properties of ochratoxin A. Spectrochim Acta Part A 2009;73(1):121–6.
[18] You JM, Lao WJ, Fan XJ, Ou QY, Jia XL. Study of the chromatographic behavior and inclusion constants of new fluorescence agents by use of cyclodextrin

additives under conditions of steady- and dynamic-state equilibrium and with fluorescence detection. Chromatographia 1999;49(1–2):95–104.
[19] Nayak MK, Dogra SK. Inter- and intramolecular excited state proton transfer in 2-hydroxy-9H-carzole-1-carboxylic acid. Spectrochim Acta Part A 2005; 61(6):1247–57.
[20] Sainz-Rozas PR, Isasi JR, Sanchez M, Tardajos G, Gonzalez-Gaitano G. Effects of natural cyclodextrins on the photophysical properties of dibenzofuran-2-carboxylic acid. J Phys Chem A 2004;108(3):392–402.
[21] Rath MC, Mahal HS, Mukherjee T. Photophysics of melatonin in different environments. Photochem Photobiol 1999;69(3):294–300.
[22] Zhou LL, Cai ZN, Yuan JY, Kang Y, Yuan WZ, Shen DZ. Multifunctional hybridmagnetite nanoparticles with pH-responsivity, superparamagnetism and fluorescence. Polym Int 2011;60(9):1303–8.
[23] Flamigni L. Inclusion of fluorescein and halogenated derivatives in alpha-cyclodextrin, beta-cyclodextrin, and gamma-cyclodextrins – a steady-state and picosecond time-resolved study. J Phys Chem 1993;97(38):9566–72.
[24] Carrier RL, Miller LA, Ahmed M. The utility of cyclodextrins for enhancing oral bioavailability. J Control Release 2007;123(2):78–99.
[25] Choudhury S, Nelson KF. Improvement of oral bioavailability of carbamazepine by inclusion in 2-hydroxypropyl-beta-cyclodextrin. Int J Pharm 1992; 85(1–3):175–80.
[26] Oteroespinar FJ, Anguianoigea S, Garciagonzalez N, Vilajato JL, Blancomendez J. Oral bioavailability of naproxen-beta-cyclodextrin inclusion compound. Int J Pharm 1991;75(1):37–44.
[27] Lao WJ, Zhang YH, Liu YQ, Wu QJ, Huang ZX, Ou QY. The microwave-assisted preparation and x-ray structure of 3-bromocarbazole-N-acetic acid. Chin Chem Lett 2001;12(4):321–4.
[28] Connors KA. The stability of cyclodextrin complexes in solution. Chem Rev 1997;97(5):1325–57.
[29] Martinez IMA, de Oca MNM, Iriarte AG, Ortiz CS, Arguello GA. Study on the interaction of Basic Violet 2 with hydroxypropyl-beta-cyclodextrin. Dyes Pigments 2012;92(1):758–65.